Analytical Methods

DOI: 10.1002/ange.201407893

# Complementary Standoff Chemical Imaging to Map and Identify Artist Materials in an Early Italian Renaissance Panel Painting**

*Kathryn A. Dooley, Damon M. Conover, Lisha Deming Glinsman, and John K. Delaney**

***Abstract:*** *Two imaging modalities based on molecular and elemental spectroscopy were used to characterize a painting by Cosimo Tura. Visible-to-near-infrared (400–1680 nm) reflectance imaging spectroscopy (RIS) and X-ray fluorescence (XRF) imaging spectroscopy were employed to identify pigments and determine their spatial distribution with higher confidence than from either technique alone. For example, Mary's red robe was modeled through the distribution of an insect-derived red lake (RIS map) and lead white (XRF lead map), rather than a layer of red lake on vermilion. The RIS image cube was also used to isolate the preparatory design by mapping the reflectance spectra associated with it. In conjunction with results from an earlier RIS study (1650–2500 nm) to map and identify the binding media, a more thorough understanding was gained of the materials and techniques used in the painting.*

The development of techniques for standoff chemical imaging enables the identification and mapping of artist materials in situ, thus offering the potential for a greater understanding of artists' working methods than from site-specific measurements alone. Such new imaging modalities utilize molecular and elemental spectroscopy. Reflectance spectroscopy in the visible and near-infrared (NIR)[1–4] or mid-IR[5,6] regions can identify and map artist materials, such as pigments and paint binders. Elemental techniques, such as X-ray fluorescence (XRF), can be used to infer the presence of inorganic materials from elemental profiles.[7] So far, no single mapping method is robust enough to identify all materials. For example, visible-to-NIR reflectance spectroscopy is hampered when distinctive spectral features are absent. In mid-IR reflectance spectroscopy, the spectral distortion from surface reflections can hinder the identification. For XRF, the elemental profile may not be sufficiently unique for pigment assignment. Thus, macroscale mapping methods are often supplemented with site-specific measurements,[1–5] whereas for microsample analysis, the use of multiple imaging modalities has become more routine.[8]

Here, we present the fusion of results from complementary chemical imaging modalities, visible-to-NIR reflectance imaging spectroscopy (RIS) and XRF imaging spectroscopy, to provide robust identification and mapping of pigments as well as the elucidation of the preparatory design in a painting by Cosimo Tura. The panel of the Virgin Mary (ca. 1475) is one of four images that comprise "The Annunciation with Saint Francis and Saint Louis of Toulouse" (Figure 1a). Each panel depicts a religious figure amid "fantastic rocky landscapes."[9]

Reflectance image cubes of the panel were collected from 400–1680 nm and registered[10] to a reference color image. Hyperspectral classification of the cubes resulted in eight reflectance spectra known as spectral endmembers (Figure 1c), which describe the majority of the painting (Figure 1b). The identification of the pigments was achieved using known spectral features.[11] XRF image cubes were collected with a spatially scanning XRF spectrometer, and elemental maps were created using the peak heights of non-overlapping characteristic emission lines (Figure 2). The combined analysis of the RIS and XRF datasets provided a robust identification of the pigments and their distribution in the painting.

The RIS endmembers display absorptions from 1400-1600 nm, assignable to the first overtone O–H stretch of gypsum (hydrated calcium sulfate),[12] and calcium (XRF map) was detected across the panel except where heavier elements suppressed the signal. These results are consistent with prior analysis that identified a gypsum ground.[3]

Red pigments used in the late 15th century include red ochre, red lead, vermilion, and red lake. In the RIS map in Figure 1b, Mary's red robe is described by the first endmember, which has strong absorption below approximately 600 nm with bands at 525 and 560 nm, consistent with an insect-derived red lake pigment.[13] The chemical structures of red lake pigments are based on anthraquinones ($C_{14}H_8O_2$), and the bands are assigned to the carbonyl $n\rightarrow\pi^*$ electronic transition. The high reflectance above 600 nm without Laporte-forbidden transitions characteristic of iron oxides[1] rules out the presence of red ochre, and the XRF map for the K$\alpha$ line of iron shows that no detectable amount of iron is present in Mary's red robe.

In historical paintings, the folds of a red fabric may consist of vermilion and/or red lead below a red lake glaze. No transition edge was found in the reflectance derivative spectra for vermilion (HgS) or red lead ($Pb_3O_4$), and XRF showed no evidence for the presence of mercury. The map for the L$\alpha$ line of lead in the red robe corresponded with the highlighted

[*] Dr. K. A. Dooley, Dr. L. D. Glinsman, Dr. J. K. Delaney
Department of Scientific Research
National Gallery of Art, 4th and Constitution Avenue NW
Washington, DC 20565 (USA)
E-mail: j-delaney@nga.gov
Dr. K. A. Dooley, D. M. Conover, Dr. J. K. Delaney
Department of Electrical and Computer Engineering
The George Washington University
801 22nd Street NW, Washington, DC 20052 (USA)

[**] The authors acknowledge support from the National Science Foundation award 1041827 and the Andrew W. Mellon and Samuel H. Kress Foundations. We thank M. Gifford, A. Hoenigswald (NGA), K. Janssens (U. Antwerp), J. Davis (NIST), D. Murphy, D. Martin, and D. Freer (SmartDrive) for support.

  

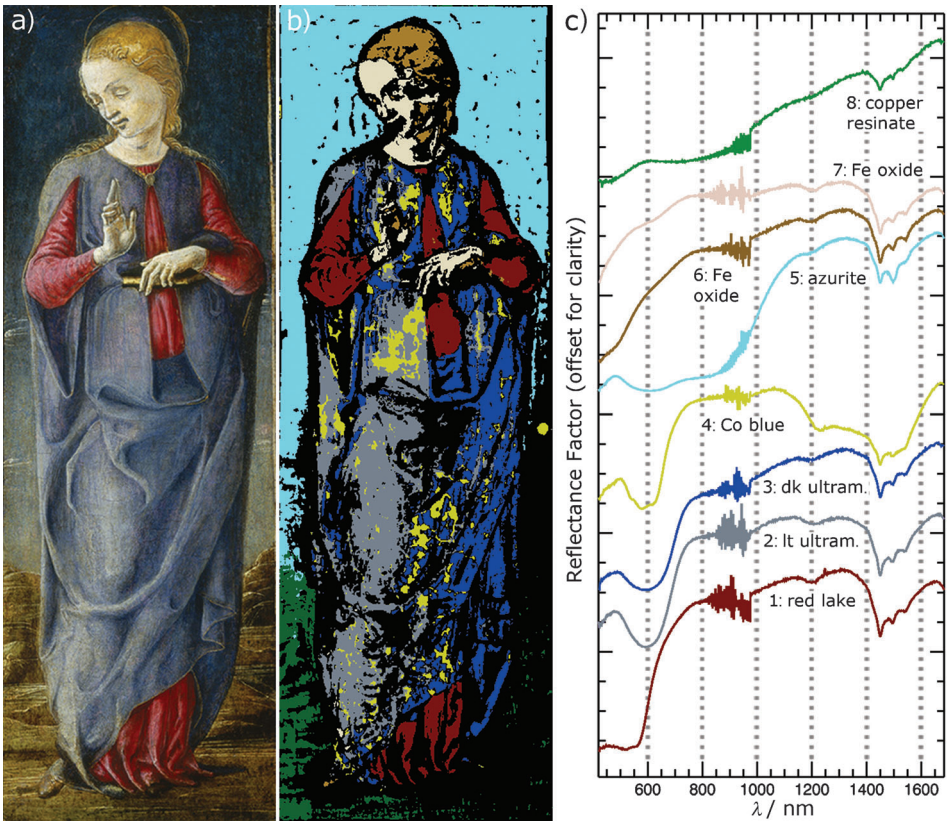


***Figure 1.*** a) Panel painting of Mary by Cosimo Tura (ca. 1470/1480, Samuel H. Kress Collection, National Gallery of Art, Washington D.C.). b) Map created with spectral angle mapping algorithm displaying spatial distributions of endmembers shown in (c). The tolerance angles (radians) for the eight endmembers are 0.105 (1), 0.09 (2), 0.085 (3), 0.145 (4), 0.165 (5), 0.07 (6), 0.1 (7), and 0.07 (8). dk = dark, lt = light.

folds. These results suggest that the red sleeves were modeled using lead white and an insect-derived red lake.

Blue pigments in the late 15th century included natural ultramarine and azurite. The second and third RIS endmembers map to Mary's blue robe and show reflectance peaks at 484 nm, broad absorption at 600 nm, and a rise in reflectance at around 700 nm, consistent with the presence of ultramarine.[14] The second endmember has a higher reflectance in the visible light region and maps to regions of the blue robe that are less saturated in color and contain a white pigment, likely lead white as the intensity of lead in the XRF map follows the spatial distribution of this endmember. The darker folds of the ultramarine robe contain less lead and match the third RIS endmember, which has a lower reflectance.

Small isolated areas of the blue robe are described by the fourth RIS endmember, which shows a reflectance peak at 440 nm and absorption at 540–640 and 1200–1530 nm. The absorption bands are indicative of d–d electronic transitions of the $Co^{2+}$ ion in cobalt blue, a modern pigment.[15] The RIS map and XRF cobalt map (not shown) match areas of known paint loss.[16]

The blue sky is described by the fifth RIS endmember with a reflectance peak at 485 nm, broad absorptions near 610 and 847 nm, and a rise in reflectance at around 900 nm. An intense absorption feature at 1497 nm overlaps with the O–H features of gypsum. These spectral features are from azurite, a basic copper(II) carbonate, $2\,CuCO_3{\cdot}Cu(OH)_2$.[17] The prior RIS binding media study also identified azurite in the sky based on NIR absorptions near 2300 nm from the OH and $CO_3$ groups.[3] This assignment is consistent with the presence of copper (Figure 2). The use of azurite for the sky and ultramarine for Mary's robe is consistent with historical practices. The color image shows a change in the saturation of the sky that corresponds to an increase in lead and decrease in copper as the horizon is approached (Figure 2). As the RIS map is a binary match to the endmembers, the spatial gradation is not seen.

Mary's hair and flesh are described by the sixth and seventh RIS endmembers, which show broad absorptions centered near 630 and 900 nm assigned to ligand field transitions of the $Fe^{3+}$ ion.[18] These features are consistent with a natural earth pigment such as ochre, which is comprised of iron oxides/oxyhydroxides. The sixth endmember, representative of a yellow iron oxide, maps mainly to Mary's hair, but also to some shadowed regions of her hands, cheek, and neck. The XRF iron map supports this assignment. The seventh endmember maps to the highlights of Mary's flesh, and is spectrally similar to the sixth endmember, but has a higher reflectance in visible regions of light, likely because a lighter-colored pigment is also present. The presence of lead white can be inferred based on the brightness of the flesh in the XRF lead map. Other pigments that may have been used for the flesh, such as umber, red lake, or vermilion, were not detected with either technique. Thus, the seventh endmember is assigned to an iron-oxide-containing pigment plus lead white and corresponds to the highlighted areas of Mary's face, neck, and hands.

The eighth endmember describes the "rocky landscape", which appears brown to the eye. The reflectance spectrum has a broad peak at about 580 nm with a gradual increase in reflectance in the NIR region, consistent with umber, which contains both iron oxides/oxyhydroxides and manganese oxides. XRF mapping shows that copper, rather than iron, best follows the contours of the brown landscape. This offers an alternative attribution of the pigment from umber to a discolored copper-containing green. Both umbers and degraded copper greens have similar reflectance spectra.[11] One potential candidate for the pigment is copper resinate, a green glaze used in Northern Italian paintings in the 15th

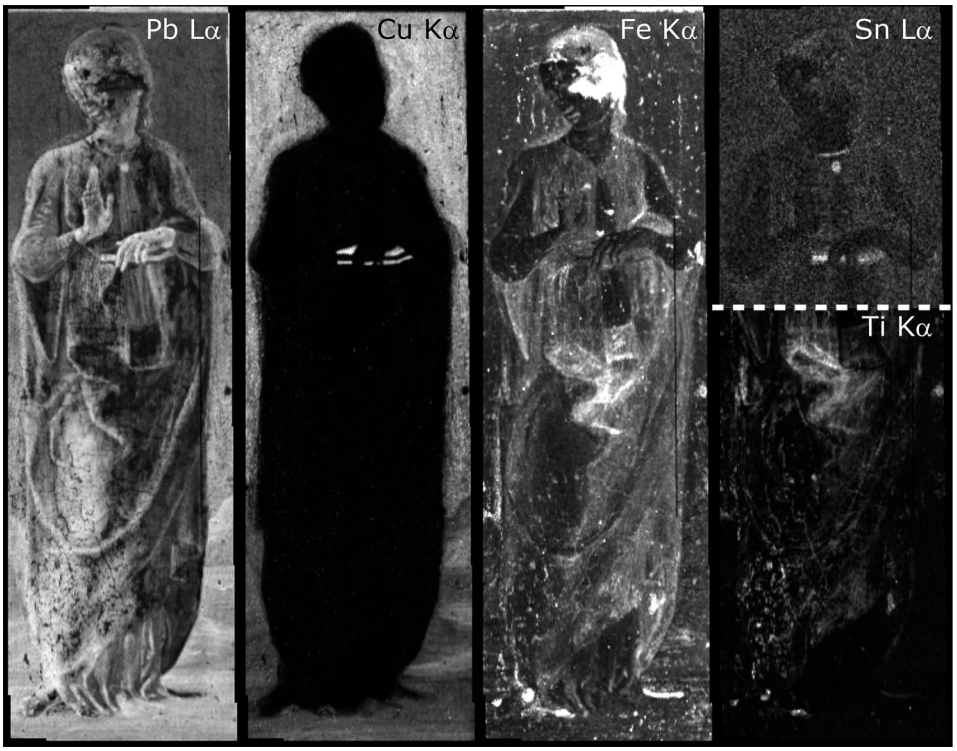


***Figure 2.*** XRF maps displaying the peak height of emission lines characteristic of the labeled elements, including the L-alpha (Lα) lines for lead (Pb) and tin (Sn) and the K-alpha (Kα) lines for copper (Cu), iron (Fe), and titanium (Ti).

and 16th centuries. A phenomenon often observed with copper resinates is a brown discoloration at the surface.[14] XRF cannot uniquely identify the green pigment, as other green pigments in use during the late 1400s contain copper (malachite and verdigris). Reflectance spectra of reference samples of malachite (copper carbonate hydroxide) and verdigris (basic copper acetate) show vibrational absorption features associated with C–O stretching[19] and C–H stretching and deformation,[20] respectively. Spectra from the brown landscape lack these absorption features. Combining the knowledge gleaned from both modalities, the pigment is assigned as copper resinate and the "fantastic rocky landscapes" were originally green.

One region not described by the computed RIS endmembers is the dark book Mary is holding. The XRF map shows the presence of copper in the book cover, which may be from malachite, as it was likely used in a similarly dark area in another panel.[3] The yellow pages of the book and the button securing her blue robe map to tin and lead in the XRF maps, consistent with the presence of lead tin yellow (not visible by RIS).

By extending RIS to include the region from 1700–2500 nm, information about the paint binders can be obtained. Prior analysis of this panel found the use of egg yolk as the binder for lead white, red lake, and iron earths and animal skin glue for ultramarine and azurite.[3]

The NIR RIS image cube also reveals information about the preparatory design, the "underdrawing" laying out the figure. The wavelengths chosen for the false-color image (Figure 3a) enhance the contrast between the underdrawing and overlying paint. In the figure of Mary, the 'brown' lines (i.e. increasing reflectance at higher wavelengths) are part of the underdrawing executed in a liquid medium, possibly with a brush.[16] These underdrawing lines emphasize the folds in the sleeves of the robe and hatching to provide shading and contrast. The 'black' regions (strongly absorbing at all three wavelengths) coincide with areas of known conservation treatment, including the middle of the blue robe and proper left side of her face. The 'black' regions map to iron (XRF map), and the middle of the robe and fill in the face also map to titanium (Figure 2) and zinc (not shown), associated with known inpaint.

Figure 3b shows the degree of match between an average NIR spectrum over an underdrawing line (red arrow, Figure 3a) and each pixel in the NIR cube. The average spectrum, shown in Figure 3c, was calculated from a region free of restoration and inpaint and overlying pigment spectral interference. In this new map, areas containing non-original paint appear less opaque. As a result, other strokes become visible and the clarity of the presumed original underdrawing is increased.

The identity of the underdrawing material is possibly umber. Some subsurface lines, such as the jawline and stroke in the middle of the neck, are visible in the XRF iron map. Not all of the underdrawing lines are visible in the iron map because the spatial samples of the scan were not optimal (see Experimental Section). Also, the NIR reflectance spectrum of the underdrawing line increases from 1000 to 1600 nm with a slope similar to umbers. Prior analysis of a cross-section from a Tura painting (National Gallery London) also found iron in the underdrawing.[21]

This study has shown that the fusion of molecular and elemental spectroscopic imaging methods through direct comparison can provide artist material assignments and maps of pigment distribution and underdrawings with higher confidence than the use of one technique alone. This dual chemical imaging approach is also expected to help when rigorous data fitting is done, by using information from one modality to constrain data fitting of the second modality. The approach is applicable to any polychrome surface, although a practical limitation is the time needed for XRF scanning, here approximately 30 times longer than RIS. Algorithms that exploit information in both modalities should help in developing automatic material classification schemes.

  


***Figure 3.*** a) NIR false-color image (R-1650, G-1250, B-1000 nm). Average reflectance spectrum of the blue robe over an underdrawing line (denoted with red arrow in (a) and solid line in (c)) maps to the dark lines in (b), hypothesized to be the original underdrawing lines.

## *Experimental Section*

Hyperspectral reflectance image cubes were collected with optimized whiskbroom line-scanning imaging spectrometers (Surface Optics Corporation). The first spectrometer utilized an EMCCD detector (Cascade II, Photometrics) operating from 380–1000 nm with 5 nm sampling, at a light level of 1100 lux and integration time of 50 ms per line. The second spectrometer utilized an InGaAs array (SUI 640SDV, Sensors Unlimited) operating from 967–1680 nm with 3.4 nm sampling, 650 lux, and integration time of 100 ms per line. The image cubes were dark-corrected, flat-fielded, and calibrated to apparent reflectance using diffuse reflectance standards (Labsphere Inc.). The calibrated image cubes were spatially registered using a point-based algorithm,[10] and the resulting spatial sampling was 0.313 mm/px. Optical fringing from 899–975 nm was minimized using a 15-channel-rolling filter and the offset difference between the image cubes was removed.

The data analysis algorithms have been previously described,[1] and ENVI image analysis software (ENVI 5.0, Exelis VIS) was used to find a basis set of spectra known as spectral endmembers. Briefly, the Minimum Noise Fraction transform calculated principal component (PC) images. The first 13 PC images were kept as the others described mainly noise. A convex geometry algorithm known as the Purity Pixel Index found a subset of pixels in the hyperspectral cube whose spectra were the most unique and diverse. These pixels were then clustered in the reduced multidimensional space defined by the number of PC images that were retained. The n-D Visualizer was used to manually select pixel clusters that were well separated. The average spectra of each cluster were the spectral endmembers. The endmembers were used to make false-color maps using the spectral angle mapping algorithm, which identified pixels in the hyperspectral cube whose reflectance spectra matched the endmember spectra within a specified tolerance angle.

XRF image cubes were collected with a scanner designed in-house using a rhodium X-ray source operating at 50 kV and 500 μA (ARTAX, Bruker AXS Inc.) with 60 μm polycapillary collimating optics, and a silicon drift detector (Vortex-60EX, Hitachi High-Technologies Science America, Inc.) operating at a peaking time of 0.5 μs and 13.7 eV sampling. The scanning was done with a high-precision 2-axis easel (SmartDrive, UK). The scan rate gave a spatial sampling of 0.5 mm/px with 100% sampling efficiency horizontally and 12% vertically. Integration time was 100 ms/px for a total scan time of 173 min, in contrast to less than 6 min total collection time for the RIS scans. The resulting XRF image cube was spectrally smoothed with a 5-channel rolling filter and registered to the color image.[10]

Received: August 2, 2014
Published online: October 15, 2014

**Keywords:** analytical methods · chemical imaging · reflectance imaging spectroscopy · vibrational spectroscopy · X-ray fluorescence

[1] J. K. Delaney, J. G. Zeibel, M. Thoury, R. Littleton, M. Palmer, K. M. Morales, E. R. de La Rie, A. Hoenigswald, *Appl. Spectrosc.* **2010**, *64*, 584.
[2] P. Ricciardi, J. K. Delaney, M. Facini, J. G. Zeibel, M. Picollo, S. Lomax, M. Loew, *Angew. Chem. Int. Ed.* **2012**, *51*, 5607; *Angew. Chem.* **2012**, *124*, 5705.
[3] K. A. Dooley, S. Lomax, J. G. Zeibel, C. Miliani, P. Ricciardi, A. Hoenigswald, M. Loew, J. K. Delaney, *Analyst* **2013**, *138*, 4838.
[4] A. Cesaratto, A. Nevin, G. Valentini, L. Brambilla, C. Castiglioni, L. Toniolo, M. Fratelli, D. Comelli, *Appl. Spectrosc.* **2013**, *67*, 1234.
[5] F. Rosi, C. Miliani, R. Braun, R. Harig, D. Sali, B. G. Brunetti, A. Sgamellotti, *Angew. Chem. Int. Ed.* **2013**, *52*, 5258; *Angew. Chem.* **2013**, *125*, 5366.
[6] S. Legrand, M. Alfeld, F. Vanmeert, W. de Nolf, K. Janssens, *Analyst* **2014**, *139*, 2489.
[7] M. Alfeld, K. Janssens, J. Dik, W. de Nolf, G. van der Snickt, *J. Anal. At. Spectrom.* **2011**, *26*, 899.
[8] K. Janssens, M. Alfeld, G. Van der Snickt, W. De Nolf, F. Vanmeert, M. Radepont, L. Monico, J. Dik, M. Cotte, G. Falkenberg, C. Miliani, B. G. Brunetti, *Annu. Rev. Anal. Chem.* **2013**, *6*, 399.
[9] M. Boskovits, D. A. Brown, *Italian Paintings of the Fifteenth Century: NGA Systematic Catalogue*, Oxford University Press, New York, **2003**.
[10] D. M. Conover, J. K. Delaney, M. H. Loew, *Proc. SPIE* **2013**, *8790*, 87900A.
[11] A. M. Baldridge, S. J. Hook, C. I. Grove, G. Rivera, *Remote Sens. Environ* **2009**, *113*, 711.
[12] G. R. Hunt, J. W. Salisbury, C. J. Lenhoff, *Mod. Geol.* **1971**, *3*, 1.
[13] C. Bisulca, M. Picollo, M. Bacci, D. Kunzelman, *9th International Conference on NDT of Art* **2008**, 1.

[14] *Artists' Pigments: A Handbook of Their History and Characteristics*, *Vol. 2*, Oxford University Press, New York, **1993**.
[15] M. Bacci, D. Magrini, M. Picollo, M. Vervat, *J. Cult. Herit.* **2009**, *10*, 275.
[16] A. Hoenigswald, NGA Paintings Conservation Report, **1997**.
[17] B. J. Reddy, K. B. N. Sarma, *Solid State Commun.* **1981**, *38*, 547.
[18] D. M. Sherman, T. D. Waite, *Am. Mineral.* **1985**, *70*, 1262.
[19] R. L. Frost, B. J. Reddy, D. L. Wain, W. N. Martens, *Spectrochim. Acta Part A* **2007**, *66*, 1075.
[20] A. Musumeci, R. L. Frost, *Spectrochim. Acta Part A* **2007**, *67*, 48.
[21] J. Dunkerton, A. Roy, A. Smith, *National Gallery Technical Bull.* **1987**, *11*, 5.

  